Model for synchronization of pancreatic β-cells by gap junction coupling

Arthur Sherman and John Rinzel
National Institutes of Health, National Institute of Diabetes and Digestive and Kidney Diseases, Mathematical Research Branch, Bethesda, Maryland 20892 USA

ABSTRACT Pancreatic β-cells coupled by gap junctions in sufficiently large clusters exhibit regular electrical bursting activity, which is described by the Chay-Keizer model and its variants. According to most reports, however, isolated cells exhibit disorganized spiking. We have previously (Sherman, A., J. Rinzel, and J. Keizer. 1988. *Biophys. J.* 54:411–425) modeled these behaviors by hypothesizing that stochastic channel fluctuations disrupt the bursts. We showed that when cells are coupled by infinite conductance gap junctions, so that the cluster is isopotential and may be viewed as a single "supercell," the fluctuations are shared over a larger membrane area and hence dampened. Bursting emerges when there are more than ~50 cells in the cluster. In the model the temporal organization of spikes into bursts increases the amplitude of intracellular calcium oscillations, which may be relevant for insulin secretion. We now extend the previous work by considering the case of a true "multicell" model with finite gap junctional conductance. Whereas the previous study assumed that the cells were synchronized, we can now study the process of synchronization itself. We show that, for sufficiently large clusters, the cells both synchronize and begin to burst with moderate, physiologically reasonable gap junctional conductance. An unexpected finding is that the burst period is longer, and calcium amplitude greater, than when coupling is infinitely strong, with an optimum in the range of 150–250 pS. Our model is in good agreement with recent experimental data of Perez-Armendariz, M., D. C. Spray, and M. V. L. Bennett. (1991. *Biophys. J.* 59:76–92) showing extensive gap junctions in β-cell pairs with mean interfacial conductance of 213 ± 113 pS. The optimality property of our model is noteworthy because simple slow-wave models without spikes do not show the same behavior.

1. INTRODUCTION

Pancreatic β-cells exhibit bursting electrical activity (sometimes called "slow waves") (Dean and Matthews, 1970) which is correlated with insulin secretion (Scott et al., 1981). Patch-clamp studies of isolated cells have characterized a number of K^+ channels and at least one Ca^{2+} channel (K-ATP: Ashcroft, 1987; K-Ca: Barrett et al., 1982; Findlay et al., 1985; delayed rectifier and Ca^{2+}: Rorsman and Trube, 1986), and a number of models have been proposed to demonstrate that the known channels can work together to generate bursts (Chay and Keizer, 1983; Sherman et al., 1988; Chay and Kang, 1988; Keizer and Magnus, 1989; Chay and Lee, 1990; Satin and Cook, 1989). At the same time there has been an effort to understand the collective behavior of cells in an intact islet of Langerhans. It is known that the cells in an islet burst synchronously, and that the cells are coupled by gap junctions, as demonstrated by both current and dye injection (Meissner, 1976; Eddlestone and Rojas, 1980; Michaels and Sheridan, 1981; Meda et al., 1984, 1986). Moreover, most investigators to date have found that single cells do not burst, but rather exhibit only irregular, apparently random, spiking (Rorsman and Trube, 1986; Bangham et al., 1986), although one recent paper does report bursts in an isolated cell (Smith et al., 1990). Finally, there is evidence that coupling enhances secretion (Halban et al., 1982; Pipeleers et al., 1982; Bosco et al., 1989).

Atwater et al. (1983) found that the conductance of a single K-Ca channel is comparable to the whole-cell conductance. They predicted that the membrane potential of single cells would be unstable, but that smooth intracellular recordings from a cell in an intact islet were the result of sharing of channels among electrically-coupled cells. Two groups of investigators (Sherman et al., 1988; Chay and Kang, 1988) used theoretical models having a finite number of stochastic channels to explore whether this "channel sharing" hypothesis could reconcile the regular bursting of islets with the irregular spiking of isolated cells. These models differed in the details of the channel kinetics, but both considered a simplified case in which the resistance of the gap junctions is zero (i.e., the conductance is ∞), and hence the entire ensemble of cells could be considered to be a single giant cell with an enlarged channel population. We will refer to these as "supercell" models.

Numerical simulations with these models lent support to the idea of channel sharing by demonstrating emergence of bursting in sufficiently large supercell clusters

Address correspondence to Dr. Arthur Sherman, National Institutes of Health, Building 31, Room 4B-54, Bethesda, MD 20892.

(~50 cells are required). As the number of cells, N_{cell}, in a cluster is increased the burst frequency decreases, the bursts become longer, and the variability of burst and active phase duration decreases (Fig. 1, *left panel*). The temporal organization of spikes into bursts also allows higher levels of intracellular Ca^{2+} to be attained (Fig. 1, *right panel*).

In this study we extend these ideas to the case in which gap junction resistance is nonzero (conductance is finite). We will refer to this as the "multicell" model. We confirm that for physiologically reasonable junctional conductance, g_c, the cells burst synchronously. In addition we report an unexpected phenomenon: the bursts can be more regular for *finite* coupling conductance than for *infinite* conductance, with lower burst frequency, less variable burst duration, and larger calcium amplitude and mean calcium. More extensive calculations show that there is a well-defined maximum in these macroscopic parameters for g_c in the range 150–250 pS, and that the multicell calculations converge to the supercell case as g_c is increased towards 1,000 pS. The theoretical optimal range of conductance per cell interface is close to the experimental value of 213 ± 113 pS obtained recently by Perez-Armendariz et al. (1991).

In Section II we present the equations for the deterministic, supercell, and multicell models and describe the relations between them. We show formally that the supercell model converges to the deterministic model as $N_{cell} \to \infty$ and that the multicell model converges to the supercell model as $g_c \to \infty$ (for N_{cell} fixed). In Section III we present the results of numerical simulations supporting the formal arguments of Section II. Some of the analysis of Section II has previously appeared in poster form and in a conference proceedings (Sherman and Rinzel, 1989). The multicell model was employed previously in a study of glucose dose-response characteristics (Carroll et al., 1990), but the model's properties were not thoroughly explored.

2. THE MODELS AND FORMAL ANALYSIS

Chay and Keizer (1983) developed a deterministic model which described the behavior of a representative β-cell during intracellular recording in an intact islet of Langerhans. Their mathematical model was based on a biophysical model proposed by Atwater et al. (1980). Several variants have been proposed using different combinations of channels, all based on the principle of fast spike dynamics modulated by a slow variable, usually free intracellular Ca^{2+}. We use the framework of the original Chay-Keizer model, as updated in Sherman et al. (1988) to include the voltage-clamp data of Rorsman and Trube (1986). The equations in outline are:

$$C_m \frac{dV}{dt} = -I_{ion}(V, n) - g_{K\text{-}Ca}(V - V_K) \tag{1a}$$

$$\frac{dn}{dt} = \lambda\left[\frac{n_\infty(V) - n}{\tau_n(V)}\right] \tag{1b}$$

$$\frac{dCa}{dt} = f(-\alpha I_{Ca}(V) - k_{Ca}Ca). \tag{1c}$$

The independent variables are V, the membrane potential, n, the open fraction of voltage-gated K^+ channels, and Ca, the concentration of free intracellular Ca^{2+}. The term $I_{ion}(V, n)$ represents the sum of the currents through the voltage-gated Ca^{2+} and K^+ channels: $I_{Ca}(V) + I_K(V, n)$.

Eq. 1a and b govern the fast spike-generating variables. The time constant of the voltage-gated K^+ channels, τ_n, was measured to be about 20–30 ms at 22°C by Rorsman and Trube (1986); τ_n/λ represents our estimate for the time constant at 37°C, where bursting is usually recorded. The effective time constant of Eq. 1a is similar to that of Eq. 1b. Eq. 1c, on the other hand, describes a slow process because f, the fraction of free intracellular Ca^{2+}, is small. The slow feedback on the spike mechanism works through the K-Ca channel conductance, $g_{K\text{-}Ca}$, which is an increasing function of Ca:

$$g_{K\text{-}Ca} = \bar{g}_{K\text{-}Ca}\frac{Ca}{K_d + Ca}. \tag{2}$$

The remaining parameters are α, a factor to convert units of current to units of concentration per time, and k_{Ca}, the rate of removal of free Ca^{2+} from the cytosol through pumping or sequestration. Eqs. 1 and 2 complete the specification of the deterministic model, except for functional forms and parameter values, which are the same as in Sherman et al. (1988). A mathematical dissection of the burst mechanism can be found in Rinzel (1985).

To account for the irregular spiking observed in an isolated cell, Sherman et al. (1988) replaced Eq. 2 with a formulation based on stochastic opening and closing of the K-Ca channels:

$$g_{K\text{-}Ca} = \bar{g}_{K\text{-}Ca}p, \tag{3}$$

where p is the fraction of channels open, and is the result of a Markov process. The transition probabilities are chosen such that the mean $g_{K\text{-}Ca}$ has the same Ca dependence as in the deterministic case:

$$\langle p \rangle = \frac{Ca}{K_d + Ca}. \tag{4}$$

The model of Chay and Kang (1988) is essentially similar, except that the site of slow feedback is Ca^{2+}-induced inactivation of a Ca^{2+} channel and the major contributor of stochastic perturbations is the voltage-dependent K^+ channel. The analysis of this paper would apply to that model equally well. A more recent proposal (Satin and Cook, 1989; Chay and Lee, 1989) is that slow feedback is the result of voltage-regulated inactivation of a Ca^{2+} channel. Again the conclusions below still follow, but the slow variable can no longer be interpreted as intracellular Ca^{2+}.

Eqs. 1, 3, and 4 model the irregular behavior of single cells. We now consider the case of coupled stochastic cells. We assume that cells are identical in size and membrane properties (but we expect that modest heterogeneity would not affect the results) and coupled by gap junctions with constant conductance g_c. Currents then flow from one cell to another in such a way as to equalize their membrane potentials: if Cell j hyperpolarizes Cell k, then Cell k depolarizes Cell j. The jth cell satisfies the following system of equations:

$$C_m \frac{dV_j}{dt} = -I_{ion}(V_j, n_j) - \bar{g}_{K\text{-}Ca} p_j (V_j - V_K) - g_c \sum_{k \in \Omega_j} (V_j - V_k) \quad (5a)$$

$$\frac{dn_j}{dt} = \lambda \left[\frac{n_\infty(V_j) - n_j}{\tau_n(V_j)} \right] \quad (5b)$$

$$\frac{dCa_j}{dt} = f[-\alpha I_{Ca}(V_j) - k_{Ca} Ca_j] \quad (5c)$$

$$\langle p_j \rangle = \frac{Ca_j}{K_d + Ca_j}, \quad (5d)$$

for $j = 1, 2, \ldots, N_{cell}$. Eq. 5 constitutes the "multicell" model. The main differences between Eq. 5 and Eqs. 1, 3, and 4 are that the variables are indexed by cell number, j, and that a term representing gap junction coupling has been added to the voltage equation. The summation in Eq. 5a is over the set of cells Ω_j to which the jth cell is coupled. In our simulations in Section III each cell is coupled to its nearest neighbors, 4 in a sheet, 6 in a cube. Edge and corner cells have correspondingly fewer neighbors. As in the supercell model, only the conductance of the K-Ca channels is treated stochastically; we expand on this point in the Discussion.

When $g_c = 0$ the cells have no influence on each other; effectively we have many copies of the single-cell equations. We sketch an argument to show that when g_c becomes very large the cells synchronize (i.e., they oscillate with the same amplitude and frequency without any phase differences). Relative to the time-scale of the *Ca* oscillations, the fast subsystem (Eq. 5a,b) instantaneously equilibrates to a steady-state solution (Rinzel, 1985). (In the silent phase the steady state is a hyperpolarized fixed voltage which depends on the instantaneous value of *Ca*, whereas in the active phase the steady state is a spikelike oscillation with a *Ca*-dependent amplitude and period.) We therefore consider the steady-state solution of the fast subsystem for g_c large and *Ca* a fixed parameter. Formally setting $g_c = \infty$ in Eq. 5a and b we find that the general solution is $V_j = \bar{V}$ for all j. In other words, the voltages synchronize. As a consequence the n values synchronize, and, over the longer time-scale of the bursts, the *Ca* values will synchronize as well. We determine the time-dependent behavior of $\bar{V}$ on the time scale of the spikes by exploiting the fact that when the V_j's are identical, $\bar{V}$ is equal to the population average:

$$\bar{V} = \frac{1}{N_{cell}} \sum_{j=1}^{N_{cell}} V_j.$$

Therefore, summing Eq. 5a over j, we have that $\bar{V}$ satisfies the equation

$$C_m \frac{d\bar{V}}{dt} = -I_{ion}(\bar{V}, n) - \bar{g}_{K\text{-}Ca} \frac{1}{N_{cell}} \sum_{j=1}^{N_{cell}} p_j (\bar{V} - V_K). \quad (6)$$

Note that the coupling terms drop out when we sum over j. The other variables, n and *Ca*, satisfy Eq. 1b and c with V replaced by $\bar{V}$. Eqs. 6, 1b, 1c, 3, and 4 are the equations for the supercell model, so-called because they are the same as the equations for an isolated, stochastic cell, but with the fraction of channels open replaced by the average of the fraction open over all the cells in the cluster.

If we now let N_{cell} get large in Eq. 6, then we expect that, because of Eq. 4, the sample paths of the stochastic system approach the solution of the deterministic equations. Our previous study (Sherman et al., 1988) verified numerically that for N_{cell} large enough (~ 50) bursts of spikes are observed instead of spikes randomly distributed in time.

Letting g_c be infinite was a simplifying assumption which allowed us to model a collection of cells as a single cell with the parameter N_{cell} representing cluster size in the voltage equation (Eq. 6). We have shown formally that the supercell model can be obtained as a limiting case of the multicell model, and that the deterministic model is a limiting case of the supercell. In Section III we study the former limiting process computationally. In addition, whereas the supercell model is applicable only to cells which are perfectly synchronized, we will now be able to study the process of synchronization itself because the multicell model is an ensemble identifiable, individual cells.

3. NUMERICAL AND STATISTICAL METHODS

The simulation algorithms used are essentially the same as in Sherman et al. (1988). Here we recapitulate some key points and describe modifications for the multicell case.

The simplest approach to the supercell problem is to solve Eq. 1 by the Euler method with time step Δt, treating the fraction p of open channels in Eq. 3 as a function of time which is determined by a separate stochastic process. Consider a single cell with $\overline{N}$ channels, N_o open and N_c closed. The mean residence times in the open and closed states, denoted τ_o and τ_c respectively, depend on Ca. During a time step the probability that one of the open channels closes is $N_o\Delta t/\tau_o$, and the probability that one of the closed channels opens is $N_c\Delta t/\tau_c$. We choose Δt such that the probabilities of these transitions are <0.1. For example, if $\overline{N} = 600$ and $\tau_c = 1$ s, Δt should be <0.167 ms. The same method works for a supercell with N_{cell} cells, but the transition rates are multiplied by N_{cell}, so Δt must be divided by N_{cell}. To solve the deterministic part of the equations accurately with the Euler method (as judged by the fact that further reductions in Δt produce little change) requires $\Delta t < 0.01$ ms. In practice it is more efficient to use the fact that the times between channel events are exponentially distributed and to choose variable length time steps with one channel event (see Sherman et al., 1988). However, the exponential method is not easy to implement for the multicell problem, so we did not use it.

The multicell case is computationally more demanding because the cells are distinct and one must compute the deterministic variables and stochastic channel processes for each of the cells, but computing time can be reduced by vectorizing the calculation over the cells. The choice of time step is subtle. First, the probability of a channel event in any given cell must be small. Additionally, one must keep small the probability that two cells in the cluster have channel events during the same time step. Otherwise, artifactual spatial and temporal summation can lead to incorrect results, especially when g_c is large and perturbations spread rapidly across the cluster. Indeed, using $\Delta t = 0.1$, which satisfies the first criterion but not the second, leads to small but systematic errors, most noticeably in the determination of minimum and maximum values of Ca. This error is substantially reduced with $\Delta t = 0.01$ ms, so we used this value for the critical summary figure, Fig. 6. With this value of Δt one can show using the binomial distribution that for a 125-cell cluster the probability of two cells having events is ~ 0.13. The probability that more than two cells have events is ~ 0.03. In comparison a 125-cell supercell would require $\Delta t = 0.0013$ ms using the simple method described above. The time courses in Figs. 3, 4, 5, 7, and 8 were computed with $\Delta t = 0.1$ ms. The CPU time for a $5 \times 5 \times 5$ cube for 100 s of model time with $\Delta t = 0.01$ ms was ~ 50 min on a Cray X-MP (Cray Research Inc., Mendota Heights, MN). For N_{cell} large (>100) CPU time is proportional to $N_{cell}/\Delta t$.

In addition to analyzing the choice of step-size, we checked the reliability of the numerical methods by verifying that simulations on another computer with a different random number generator and with different geometries (one-, two-, and three-dimensional; periodic and no-flux boundary conditions; different cluster sizes) all produced similar results.

We quantitatively study the effects of N_{cell} and g_c on bursting by collecting statistics on several macroscopic parameters. We first locate the maxima and minima of Ca. Because Ca is a slow variable much of the stochastic fluctuation is smoothed out, and we do some additional smoothing by taking a rolling average of a few neighboring points. From the extrema we determine the beginning and ending of each active and silent phase. (This procedure is robust for $N_{cell} \geq 10$ for the supercell and $g_c \geq 35$ pS for the multicell where bursts can be distinguished from brief transient fluctuations.) For each statistic we compute the sample mean (μ) and sample standard deviation (s) over a run of 100 s (multicell) or 200 s (supercell). The sample size (n) therefore depends on the burst period, with more samples being taken in the noisier, shorter period cases. For the supercell, n decreases from 73 at $N_{cell} = 10$ to 10 at $N_{cell} = 400$. In the multicell case, there is also variability among cells withing a cluster, so we average over the five cells along a diagonal to obtain a single representative value. The number of bursts in 100 s ranged from five at the peak of the burst period curve (Fig. 6) to 11 at the extremes. To compare the "noisiness" of different cases we looked at the coefficient of variation (COV = s/μ) to take into account the changes in burst duration.

Because each simulation gives only one realization of the stochastic process we estimate the variation in the computed means between different realizations due to the small sample size by the standard error of the mean (SEM = $s/\sqrt{n}$). Comparing runs with different seeds for the random number generator for selected cases gave differences less than twice the SEM. Typical values of the SEM relative to μ in Figs. 2 and 6 were 5% for T_B, 0.8% for the maximum of Ca, and 0.2% for the minimum of Ca. The small sample size is responsible for the unevenness seen in Fig. 6; we assume that the true underlying curves of burst period and maximum Ca are smooth with a single maximum while the curve of minimum Ca is monotonic.

4. RESULTS OF NUMERICAL SIMULATIONS

For purposes of comparison with the multicell model we have included some computations with the supercell for various values of N_{cell} (Fig. 1, *top three panels*) and with the deterministic model (Fig. 1, *bottom*). As N_{cell} increases bursting appears, accompanied by oscillations in *Ca*. In Fig. 2 we have plotted the average burst duration (*top*) and the average minimum and maximum *Ca* (*bottom*), calculated as described in the methods section. Burst period and peak-to-peak *Ca* amplitude increase monotonically with N_{cell}. The maximum *Ca* increases and the minimum *Ca* decreases towards the values of the deterministic model. We also find that active phase percent (measured as relative time for *V* above a threshold, not shown) is approximately independent of N_{cell}. This means that spike frequency, averaged over long times, is independent of N_{cell}, but temporal summation allows increased *Ca* accumulation as the spikes cluster into bursts.

Fig. 3 shows numerical simulations of the multicell model for a 2 × 2 × 2 cube and a 5 × 5 × 5 cube at low

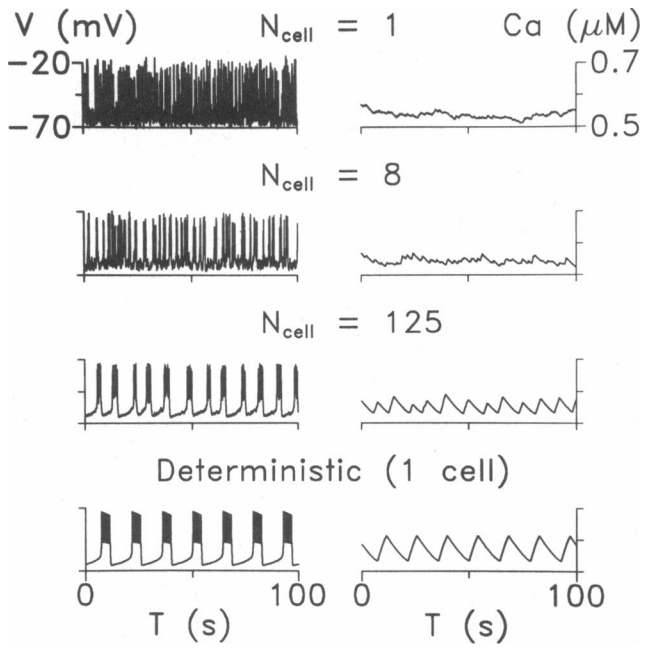

FIGURE 1 Membrane potential (*left*) and free intracellular calcium (*right*) for stochastic supercell model ($g_c = \infty$) with 1, 8, and 125 cells; numerical simulation of Eqs. 6, 1b, 1c, 3, and 4. As the number of cells, N_{cell}, increases the spikes become organized into bursts and sawtooth oscillations develop in intracellular calcium. Same parameters except for N_{cell} as in Fig. 8, Sherman et al., 1988. As N_{cell} increases the solutions begin to approximate those of the single cell deterministic model (Eqs. 1 and 2), shown in the bottom panel.

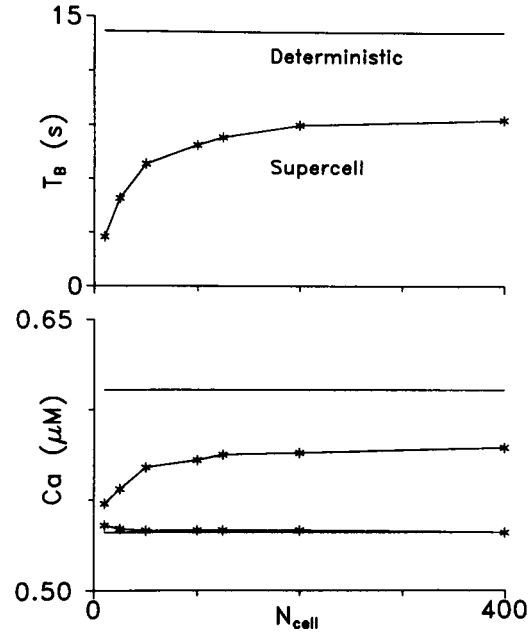

FIGURE 2 (*Top*) In the supercell model burst period (T_B) increases with N_{cell} and approaches the value for the deterministic model (*solid line*). (*Bottom*) Correspondingly, the minimum and maximum values of the sawtooth *Ca* oscillations approach the deterministic threshold values (*solid lines*). T_B and *Ca* values are calculated from simulations of 200 s and averaged. The number of bursts ranged from 10 to 73.

(25 pS) and high (175 pS) coupling conductance. For both the small and large cubes there is an increase in the degree of synchronization, the bursts become more ordered in appearance, and burst period increases when g_c is increased from 25 to 175 pS. With only eight cells the bursts remain short and variable, whereas with 125 cells the bursts become long and regular. Thus, both sufficiently many cells and sufficiently strong coupling are needed to obtain regular bursts. It is difficult to define a precise value of g_c at which bursting first appears because the spike pattern gradually becomes more and more regular, but in the 5 × 5 × 5 cube bursting is well established at $g_c = 50$ pS.

A striking observation is that the 5 × 5 × 5 cube with $g_c = 175$ pS has longer burst period than the supercell (Fig. 1, $N_{cell} = 125$) and even slightly longer than the deterministic case (Fig. 1, *bottom*). Fig. 4 shows that the peak *Ca* and the peak-to-peak *Ca* amplitude are also larger for the multicell case. The burst durations are more uniform for the 5 × 5 × 5 cube than for the 125-cell supercell as measured by the COV (see methods): 0.08 for the multicell vs. 0.23 for the supercell. The 2 × 2 × 2 cube similarly has longer bursts and higher *Ca* amplitude than the 8-cell supercell.

The above holds even though the multicell simula-

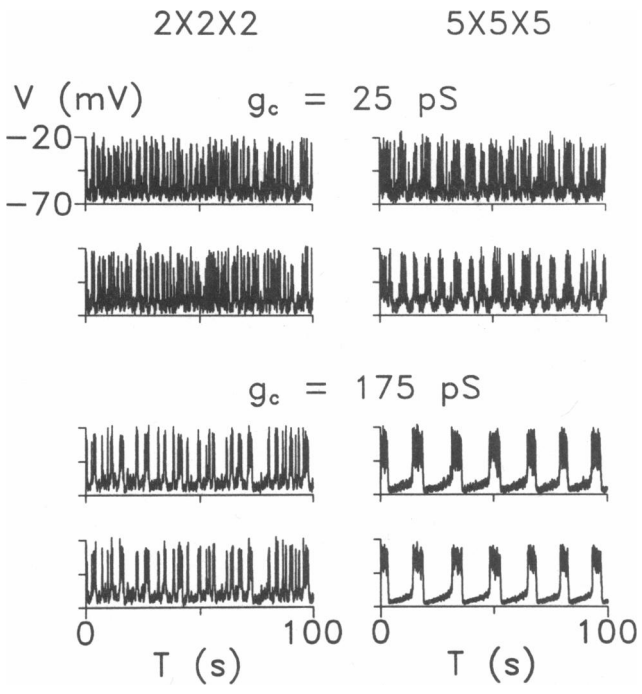

FIGURE 3 Membrane potential time courses for the multicell model for two cells selected from a 2 × 2 × 2 cube (*left panels*) and a 5 × 5 × 5 cube (*right panels*). Numerical solution of Eq. 5, parameters as in Fig. 1. In the 5 × 5 × 5 cube the upper record is from a corner cell and the bottom record is from the center cell. Regular bursting with long active phases requires both adequate coupling conductance, g_c, and adequate population size, N_{cell} (*bottom right*).

tions have more silent phase noise than the supercell. This is one aspect of an interesting dichotomy between the long and short time scale behavior of the multicell as compared to the supercell. To examine this more closely we have plotted some voltage time courses for the 5 × 5 × 5 cube on an expanded time base in Fig. 5.

At g_c = 10 pS, the corner cell (Fig. 5, *upper panel*) and the center cell (Fig. 5, *lower panel*) appear to be completely uncorrelated. The spikes are large in amplitude with little evidence of a plateau. The long time scale records (not shown) are essentially the same as the 1-cell supercell (Fig. 1, *top*). At g_c = 25 pS there is some evidence of bursting in synchrony, but it is difficult to distinguish silent phase noise from bona fide bursts. There is a large voltage excursion at $t \approx 0.5$ s in the corner cell which has failed to propagate to the center cell. At g_c = 175 pS, the burst initiation is very synchronous, but the spikes are not synchronized. The spike amplitude is much smaller and the frequency is much higher than in the supercell (Fig. 5, *bottom left*) or the deterministic cell (Fig. 5, *bottom right*). This reflects a change in the solutions of the underlying deterministic equations when coupling is not too strong (see Discussion). At g_c = 2,000 pS the spikes are almost perfectly synchronized and their appearance is qualitatively identical to that of the supercell, as is that of the long time scale records (not shown). This case illustrates the convergence of the multicell to the supercell which was predicted by the formal analysis in Section II.

A final view of the relation between the multicell and the supercell is afforded by Fig. 6, where we study the parametric dependence of burst period, T_B, and minimum and maximum *Ca* on coupling conductance, calculated as described in the methods section. Burst period and peak-to-peak *Ca* amplitude increase with g_c at first, reach a maximum near 150–250 pS, and then decrease towards the values corresponding to the supercell. The coefficients of variation (not shown) fall into two groups: the COV averaged over values of g_c for g_c between 50 and 375 pS is 0.08; for $g_c \geq 500$ pS the average is 0.21, comparable to the supercell.

In the 2 × 2 × 2 case as well (not shown) increasing g_c to very large values does not lead to longer and longer bursts, but rather to voltage and calcium time courses which are indistinguishable from those of the 8-cell supercell.

Thus, we have the paradox that the multicell is more noisy than the supercell when we consider fast time-scale fluctuations in the spikes and silent-phase potential, but less noisy when we consider the slow waves. Furthermore, the low-frequency slow waves synchronize at relatively low coupling strength, whereas the high-frequency spikes are out of phase. This is due to the fact that high frequency perturbations decay more rapidly with distance, provided the dimensions of the cluster are

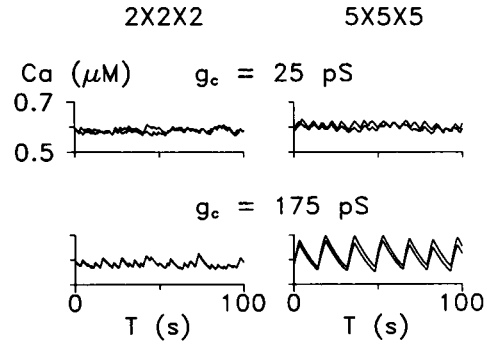

FIGURE 4 Calcium oscillations for the multicell model for the same cells depicted in Fig. 3. To save space, the results for two cells are shown superimposed for each case. As in the supercell model, *Ca* oscillations develop as the bursts become more regular. Note that in the bottom right case, peak-to-peak *Ca* amplitude is greater than both the supercell with N_{cell} = 125 and the single-cell deterministic case (Fig. 1, *bottom*).

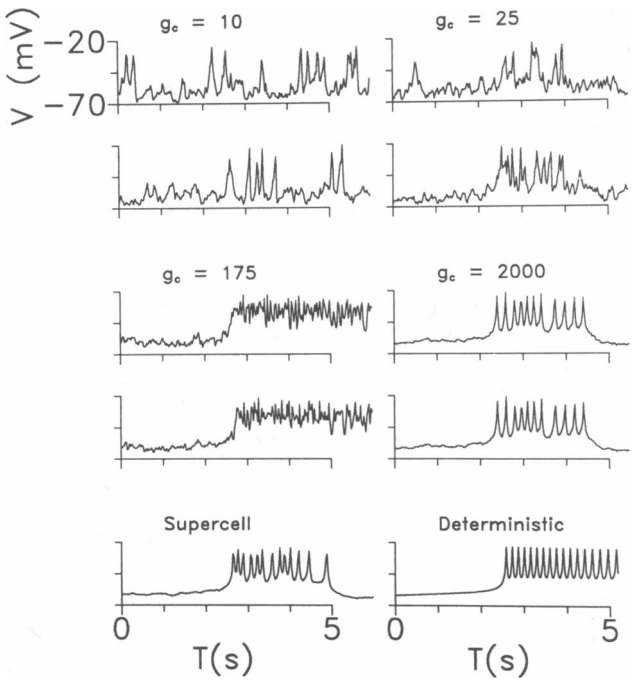

FIGURE 5 Spikes are shown on an expanded time base (5 s) for a 5 × 5 × 5 multicell at four values of coupling conductance, for a 125-cell supercell, and for a single deterministic cell. In the multicell panels the upper traces are from a corner cell, and the lower traces are from the center cell. Panels for g_c = 25 and 175 pS are taken from the same simulations as in Fig. 3. Bursts synchronize at much lower values of g_c than spikes; synchronized spiking coincides with convergence of the multicell to the supercell.

sufficiently large (Rall, 1976; see also Rall and Segev, 1985, Fig. 4). Only at very high values of g_c do the individual spikes synchronize, corresponding to the regime where burst duration and *Ca* amplitude fall towards the supercell values in Fig. 6. Thus, even though some synchronization is necessary for bursting to occur, too much synchronization reduces burst duration and *Ca* amplitude and increases variability. Resolving these apparent paradoxes requires exploration of the underlying dynamics of bursting, which we defer to the Discussion.

Having a model in which distinct, individual cells are represented allows us to simulate the two-electrode experiments of Eddlestone et al. (1984) in which simultaneous intracellular recordings were taken from two cells. They found that even widely separated cells in an islet have synchronized bursts, but that current injected in one cell caused voltage deflections only in cells less than a few cell diameters away. We find the same features. Fig. 7 shows the injection of 500 ms, 20 pA current pulses at 1 Hz into the center cell of a 5 × 5 × 5 cube with g_c = 175 pS. Although the cluster experiences two synchronized bursts and the burst pattern is almost obliterated in the injected cell (Fig. 7, *upper time course*), only the nearest neighbors (Fig. 7, *middle time course*) of the injected cell show significant voltage deflections. Cells more than two neighbors distant are only slightly perturbed (Fig. 7, *bottom time course*). The bottom panel indicates the spatial profile of membrane potential at the end of the silent phase before the second burst (t = 12.85 s, indicated by arrow above upper time course), showing sharp attenuation. A similar profile is found during the bursts, but with a higher mean potential level and more scatter because the spikes are unsynchronized. Along the silent phase an increase in input resistance due to closing of K-Ca channels is visible, followed by a decrease as the active phase begins; both of these features are seen experimentally in intracellular recordings (Atwater and Rinzel, 1986). The spatial rate of decay of voltage does not vary much from the silent phase to the active phase because the changes in input resistance are relatively small, but as g_c is increased towards 1,000 pS the spatial profile of poten-

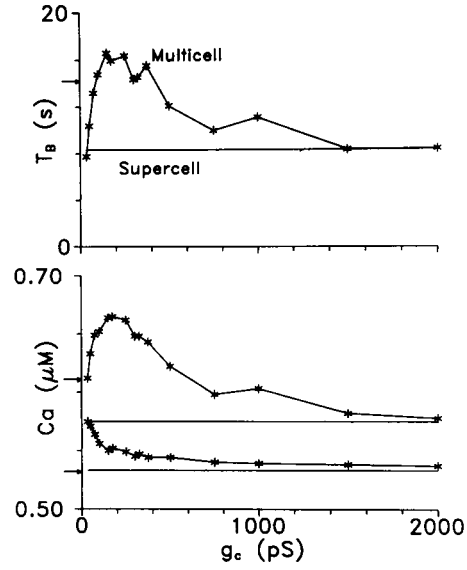

FIGURE 6 (*Top*) For the 5 × 5 × 5 cube (multicell model), burst period first increases, then decreases with increasing coupling conductance with a maximum at g_c = 175 pS. Burst period approaches that of the 125-cell supercell (*solid line*) for very large g_c. (*Bottom*) Time-averaged *Ca* minima and maxima lie above the corresponding values for the 125-cell supercell (*solid lines*), decreasing towards the supercell values for very large g_c. There is a range of g_c values for which peak *Ca* and T_B are greater for the 5 × 5 × 5 cube than for the single-cell deterministic case (Fig. 1); deterministic values are marked by arrowheads on ordinate. T_B and *Ca* values are means averaged over a 100 s run (5–11 bursts) for each of the five diagonal cells, and then averaged over the cells as described in Methods.

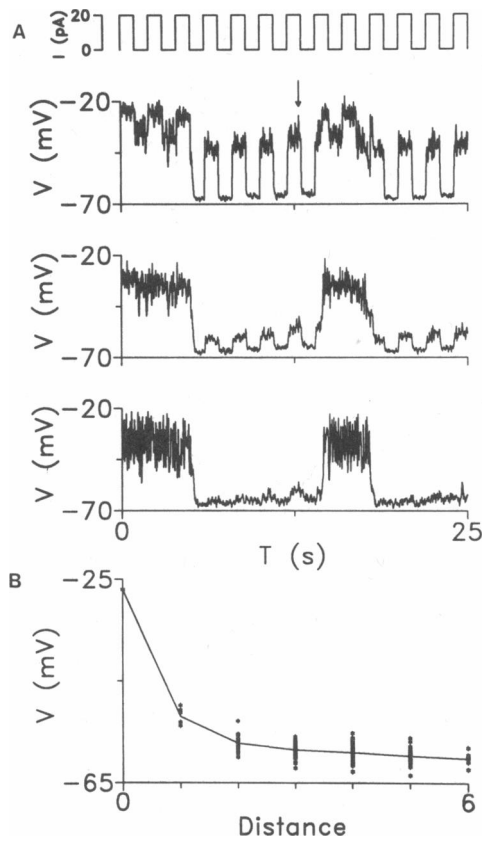

FIGURE 7 Simulation of injection of 0.5 s 20 pA current pulses into the center cell of a 5 × 5 × 5 cube. Coupling conductance is 175 pS. (*A*) Membrane potential time course for the injected cell (*top*), for a cell which is an immediate neighbor of the injected cell (*middle*), and for a corner cell (*bottom*). (*B*) Membrane potential plotted against distance (measured as minimum path length) from the center cell, corresponding to t = 12.85 s in *A*, indicated by arrow. Stars represent each cell and the solid line represents the mean over cells at a given distance. Cells more than about two links distant have negligible deflection.

tial becomes flat, with a large decrease in the size of the deflection at the injection site.

It is interesting that we find optimal burst period when the spatial voltage profile is still rather sharply peaked. In one of the early experimental studies of gap junction coupling in islets (Atwater et al., 1978) the rapid spatial fall off of voltage perturbations led to skepticism about the role of gap junction coupling in synchronization of islets. Our simulations, however, show that short-range influence of individual cells can bring about long-range order.

In the case of Fig. 7 no cell is more than six links away from the center of the cluster, but we find similar behavior in larger clusters (eg., 32 × 32), where we also observe phase lags of ~1–2 s as seen experimentally (Eddlestone et al., 1984; Meda et al., 1984; Valdeolmillos et al., 1989). Meda et al. (1984) found that the more central cell led the more peripheral cell ~60–70% of the time. By visualizing the voltage in the entire ensemble (Fig. 8) we can see that, in the model, the phase lags are due to waves of burst depolarization and repolarization arising in random locations and traveling across the cluster. If one had only two electrodes, measurement of relative phase would be highly dependent on the particular cells impaled and it might be difficult to determine whether the inner or outer cells were leading on the whole. Stokes and Rinzel (manuscript in preparation) have found systematic phase lags with the edge leading in a model in which cells are coupled through extracellular variations in $[K^+]$.

In simulations like that shown in Fig. 8 where the boundary cells have fewer neighbors than the interior cells, the traveling waves usually begin at the corner (and occasionally the edge) cells. This is because corner cells have higher input resistance, and hence can more easily achieve large voltage differentials from the ensemble average. Note that in Figs. 3 and 5 the corner cells are noisier than the center cells (except when g_c is so large that the cells are perfectly synchronized). When edge effects are eliminated by using periodic boundary conditions the traveling waves appear to start anywhere in the ensemble with equal probability. We have not attempted to accurately represent the true boundary conditions in a pancreatic islet. For example, the surface cells in an islet

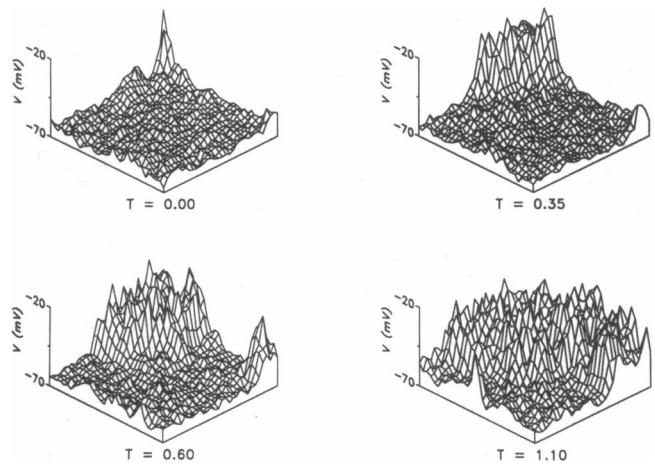

FIGURE 8 Initiation of an active phase in a 32 × 32 sheet of cells. Coupling conductance is 175 pS, f = 0.002 which means burst frequency is roughly double that in previous figures; other parameters are unchanged. t = 0: a wave of depolarization begins in the upper corner. t = 0.35, t = 0.60: a secondary wave begins independently in the right corner. t = 1.10: the two waves merge. By t = 1.60 (not shown) the wave has filled the entire sheet.

are mostly nonbursting α and δ-cells. Also, boundary effects may be less important in large islets with a small surface-to-volume ratio.

5. DISCUSSION AND INTERPRETATION

We have extended previous work (Sherman et al., 1988) on the role of gap junction coupling in simultaneously synchronizing electrical activity within pancreatic islets and organizing that activity into bursting oscillations. We have situated the previous deterministic and supercell models and the new multicell model within a two-parameter continuum defined by the coupling conductance, g_c, and the number of cells, N_{cell}. The coupling strength determines the degree of synchronization whereas the number of cells sets an upper limit to the degree of temporal organization of the collective activity. If cell membrane currents are noisy, as we assume, both adequate coupling and adequate ensemble size are required to achieve regular bursting: temporal organization cannot occur in the absence of synchronization (Fig. 3). We have shown that the perfect coupling assumed in our previous study is not required to attain synchronized bursting. Indeed, moderate coupling, which synchronizes the bursts but not the spikes, maximizes the amplitude of intracellular Ca^{2+} oscillations and burst period. We hope that ways can be found to selectively adjust gap junctional conductance in islets or in clusters of cultured cells of various sizes in order to test these predictions.

What is the significance of gap-junction coupling for insulin secretion? We know that coupling enhances secretion (Halban et al., 1982; Pipeleers et al., 1982; Bosco et al., 1989) and we know that influx of extracellular Ca^{2+} is necessary for secretion (Boyd et al., 1989). Our model shows that coupling leads to intracellular Ca^{2+} oscillations via bursting, but it does not yet allow us to say anything about the effects of coupling on the internal secretory processes of β-cells or effects due to sharing of organic molecules; we have only studied the role of gap junctions in equalizing membrane potential. Further work is also needed to investigate the possible role of reciprocal interactions between pulsatile Ca^{2+} influx through the membrane, the Ca^{2+}-handling machinery, and metabolic processes.

Comparison with experiment

Investigators have long wondered whether gap junctions are responsible for synchronization of bursting in islets because current injected in a cell decays within a few cell diameters (Atwater et al., 1978; cell diameter ≈ 10–15 μm) while burst synchrony has been demonstrated between cells in intact islets up to 400 μm apart (Meda et al., 1984). Moreover, injection of Lucifer yellow dye usually stains only two to five neighboring cells (Meda et al., 1986). Direct electrical measurements of β-cell pairs from freshly dispersed islets (Perez-Armendariz et al., 1991) found that 65% of cell pairs were electrically coupled and that electrical coupling can exist even when dye coupling does not. The value 65% may either understate the value in an intact islet (if cell contacts are disrupted in the dispersal process) or overstate it (if cells which were connected in the islet preferentially survive dispersal).

These are difficult questions to answer definitively. Our modeling has shown that if all cells are coupled by gap junctions (or, presumably, if coupling is sufficiently extensive) then large cell clusters can be burst-synchronized by physiologically reasonable conductances. The junctional conductances between cell pairs found experimentally lie mostly in the range 100–300 pS, which corresponds well to the values which give optimal burst period and *Ca* amplitude in our model. We have also shown that the synchronization process does not require a pacemaker and that even short-ranged local interactions (Fig. 7) can give rise to waves of depolarization and repolarization that spread and produce global synchronization with small phase lags (Fig. 8). An interesting subject for future work is to investigate how much our conclusions would be modified if only some fraction of cells were coupled.

Another limitation of our study is that even with supercomputing techniques we have had to limit our statistical convergence study to a relatively small ($5 \times 5 \times 5$) cell cluster. From the formal theory of Section II one expects that, independent of N_{cell}, the behavior of a multicell cluster will shift from chaotic spiking to that of the corresponding supercell as g_c increases, and that larger g_c will be required to synchronize larger clusters. Preliminary study of a larger ($11 \times 11 \times 11$) cluster confirms these predictions, and indicates that there is an optimum in T_B, but with a substantially broadened peak. Burst period exceeds that of the supercell for g_c between 100 pS and at least 1,000 pS (i.e., including the entire physiological range), with an optimum probably near 500 pS.

For simplicity we have treated the gap junctions as voltage and time-independent conductances, although there is evidence in some preparations for stochastic openings similar to standard channels. We note, however, that Perez-Armendariz et al. (1991) found that the junctional conductance did not vary with time or voltage and did not exhibit channel gating within the resolution (20 pS) of their measurements. Sherman et al. (1988)

and Chay and Kang (1988) found for their supercell models that it was adequate to consider the stochastic fluctuations of only the largest membrane channel, with our parameters the K-Ca channel at 50 pS. It remains to be determined how much stochastic fluctuation in junctional conductance would be required to substantially inhibit burst synchronization.

We have also not explored the possible effects of cell inhomogeneity or systematic spatial variation of cell properties: all of our cells are identical. For example, it is known that cells in the islet are segregated, with bursting β-cells in the interior and a thin layer of nonbursting α and δ-cells in the periphery.

One must consider the possibility that gap junctions do not bear sole responsibility for synchronization. The finding of only small dye-coupled clusters of cells has led to speculation that gap junctions create small islands of tightly coupled cells (Orci, 1982) and that these islands are synchronized by a different coupling mechanism, such as diffusion of K^+ in the extracellular space (Perez-Armendariz et al., 1986). Stokes and Rinzel (manuscript in preparation) have shown that K^+ diffusion can synchronize cell clusters, at least in the case where the oscillators are identical and determinstic (i.e., channel noise is negligible).

There is still controversy over what is the precise mechanism of bursting, which raises the question of how much our results about coupling depend on the choice of underlying model. All the models proposed to date have been based on feedback of a slow variable on a fast spiking mechanism. In most of the models this feedback role has been played by free intracellular Ca^{2+}, either by activating K-Ca channels (Chay and Keizer, 1983, Sherman et al., 1988) or ATP-blockable K^+ channels (Keizer and Magnus, 1989), or by inhibiting Ca^{2+} channels (Chay and Kang, 1988). The mathematical structure of all of these models is essentially the same and fits in the paradigm of the fast-slow analysis of Rinzel (1985); only the labels of some of the variables need to be changed. We are confident that our coupling results hold qualitatively for all of these models. Quantitatively there may be differences in features such as the optimal value of g_c. We expect, however, that if the degree of channel noise is similar, the optimal g_c would be comparable to the whole-cell conductance.

Recently the first measurements of intracellular Ca^{2+} oscillations in bursting β-cells have been reported (Valdeolmillos et al., 1989); the Ca^{2+} oscillations coincide in time with bursting electrical activity (Rosario et al., 1990). They do not have the sawtooth shape predicted by the Ca^{2+} feedback models; Ca^{2+} rises rapidly at the beginning of a burst to a plateau and decays slowly once the burst ends. This casts doubt on the idea that intracellular Ca^{2+} is a slow variable. One alternative proposed by Satin and Cook (1989) and Chay and Lee (1990) is that voltage-inactivation of a Ca^{2+} channel is the site of slow feedback. Further work is needed to resolve these questions, but we expect that our coupling results would apply: there would be an optimum in T_B and in the amplitude of the slow inactivation variable. There would not be an optimum in *Ca* amplitude, but there would be one in the duration of the plateau.

Although previous investigators (Rorsman and Trube, 1986; Bangham et al., 1986) have found only irregular spiking as the typical situation in isolated β-cells, Smith et al. (1990) have recently reported bursts in single mouse β-cells using perforated patch whole-cell recording at 30°C. The previous measurements were done with whole-cell patch clamp at 20–22°C. It is therefore possible that the channel noise which we incorporate in our model is an artifact of low temperature, cell injury, or dialysis of cell interior with the electrode medium. We note that another recent study (Falke et al., 1989) using the perforated patch technique found glucose-dependent spiking, but not bursting, in isolated rat β-cells at room temperature. Applying the same technique to surface cells of intact human islets they recorded bursts with a period of 2–10 s, comparable to the values obtained historically by intracellular recording in intact mouse islets and much shorter than those reported by Smith et al. (1990) (1–4 min). It is possible that Smith et al. (1990) are observing not bursts, but the effects of much slower intracellular processes. For example, Grapengiesser et al. (1988) found cytoplasmic Ca^{2+} oscillations in isolated cells with a period of 2–6 min and Henquin et al. (1982) and Cook (1983) measured modulations of bursting activity in islets with similar periods. Valdeolmillos et al. (1989) found some mouse islets with slow Ca^{2+} oscillations modulating more rapid Ca^{2+} oscillations, the latter likely coinciding with bursting electrical activity.

Our model does not address phenomena on the several-minute time scale, but we have used it to explore the effects of gap-junction coupling in the absence of channel noise by multicell simulations in which each cell is deterministic. Not surprisingly the cells synchronize, but we also find that for g_c between 10 and 150 pS the burst period is 60% longer than for a single deterministic cell. *Ca* amplitude is more than doubled compared to a single cell. As g_c is made larger the burst period and *Ca* amplitude decrease back to the deterministic single cell values. Thus, even if single cells can burst, coupling is required for synchronization, and moderate gap junctional conductance yields optimal levels of burst period and *Ca* amplitude.

Why is there an optimal coupling strength?

To understand why there is an optimum value of g_c for the stochastic multicell model (Fig. 6) we must review briefly the mechanism of switching from active to silent phase in the deterministic and supercell models.

In the deterministic case, phase switching occurs when *Ca*, or equivalently, $g_{K\text{-}Ca}$, reaches a lower threshold (for the initiation of the active phase) or an upper threshold (for the termination of the active phase). See Fig. 1, bottom. In the supercell and multicell models $g_{K\text{-}Ca}$ is stochastically decoupled from *Ca* (Eq. 3), and channel fluctuations cause $g_{K\text{-}Ca}$ to jump back and forth across the deterministic thresholds (Sherman et al., 1988, Fig. 9). It is thus difficult to characterize the conditions for phase switching to occur, but simulations show that it is usually premature, resulting in a short burst period. For the supercell, as N_{cell} gets large the population average of $g_{K\text{-}Ca}$ follows the mean determined by *Ca* more closely (Eq. 4), phase switching occurs closer to the deterministic thresholds, and burst period increases (Fig. 2).

Now consider the multicell case with N_{cell} fixed and g_c increasing. As in the supercell, the population average of $g_{K\text{-}Ca}$ roughly controls when phase switching occurs, but now fluctuations can accumulate locally. By simulating the injection of current into individual cells we have found that the islet is insensitive to local fluctuations when the average $g_{K\text{-}Ca}$ is far from threshold, but near threshold a local fluctuation can grow into a wave that switches the phase of the entire islet. We see this occurring spontaneously in Fig. 8. As g_c increases, the space constant (i.e., the distance for an *e*-fold decay in membrane potential; Rall, 1977) increases and the islet becomes less sensitive to these local fluctuations because they are shared over a larger region (i.e., the conductance load increases). This accounts for the increase in burst period and *Ca* amplitude for g_c increasing in the range < 150 pS in Fig. 6.

If the above were the only mechanism at work, we believe that the supercell would always have longer burst period and that the multicell burst period would increase monotonically with g_c to that of the supercell. This is indeed the convergence pattern we find when we couple slow wave oscillators such as the Fitzhugh-Nagumo model (Fitzhugh, 1961), which have nonspiking plateaus rather than spiking active phases. In the case of the β-cell (Eqs. 1 and 2) and other oscillators with similar dynamic structure, however, the bursting solution obtained with a single deterministic unit may become unstable when such units are coupled. A new solution with higher upper threshold, longer burst period, and higher maximum *Ca* appears. (The lower threshold of the coupled deterministic units is unaffected, however. Indeed, in Fig. 6 the minimum *Ca* for the multicell is further from the deterministic threshold than that of the supercell, and decreases monotonically with g_c, unlike maximum *Ca*.) A key feature of this new solution is that the bursts are synchronized, but the spikes are out of phase. This bifurcation to out-of-phase spiking is a *deterministic* phenomenon, but it establishes a new threshold which influences the phase switching of the stochastic simulations. For g_c sufficiently large the out-of-phase behavior disappears and the standard in-phase solution restabilizes. That is what accounts for the decrease in burst period and *Ca* amplitude for g_c larger than 250 pS in Fig. 6. The in-phase solution reappears because the cells are perfectly synchronized when the coupling is infinitely strong, and thus can not spike out of phase. The deterministic out-of-phase solution is also characterized by smaller amplitude, higher frequency spikes, a feature which carries over to the stochastic case when g_c is large enough to allow regular bursting but not so large that the cells are pefectly synchronized (Fig. 5, $g_c = 175$ pS).

Comparison to other systems

There are many physical and biological systems that feature coupling by diffusion, and this study may be of general interest. In biology, gap junctions are frequently found where coordinated behavior is required. We have considered identical oscillators which desynchronize in the absence of adequate coupling strength because of channel noise. Other theoretical models have considered noise-free oscillators which have different intrinsic frequencies. Typically, for strong enough coupling, the oscillators phase lock at an intermediate frequency. An example of this is the work of Michaels et al. (1986) on electronically-coupled pairs of mammalian sinoatrial (SA) pacemaker cells. In contrast we find that, if the coupling is not too strong, our cells oscillate more slowly than their common uncoupled frequency.

Michaels et al. (1987) have also simulated the central pacemaker region of the SA node as a sheet of coupled oscillators with frequencies randomly assigned by applying different bias currents. For sufficiently large coupling conductance the ensemble entrains at an intermediate frequency, with phase lags. They refer to this as a "democratic" process because the collective frequency is not just the frequency of the fastest cell as in the classical view of pacemaking. Some cells are "more equal than others," however, because the wave of depolarization spreads from a consistent focus. In our model the timing of active and silent phase initiation is also determined by a collective averaging process, but

the site of initiation wanders randomly from burst to burst. We suspect that the initiation site in the SA model is a group of neighboring cells with higher than average frequencies, so that it may perhaps be more properly described as an "oligarchy" than a "democracy."

The slowing of our oscillators by coupling depends on the existence of a stable out-of-phase solution. We are aware of one other physical example in which this occurs. Crowley and Epstein (1989) coupled two stirred chemical reactors by mass flow through ports in the walls and found a bifurcation to an out-of-phase oscillation experimentally. The same behavior was obtained in a theoretical model. As in our model, the frequency of the out-of-phase solution is lower than the intrinsic frequencies of the uncoupled reactors. Sufficiently strong coupling destabilizes the out-of-phase solution and leads to in-phase oscillations. Their model, however, has a different dynamic structure than ours and exhibits some distinct phenomena, such as annihilation of oscillations by strong coupling.

A question that arises is whether other types of cell coupling, such as synaptic transmission, can exhibit similar behavior. We are currently investigating simplified, low-dimensional deterministic models to understand the essence of this phenomenon and find out how general it may be.

We thank Daniel Kaplan of Massachusetts Institute of Technology for pointing out the oligarchical nature of the Michaels model.

We acknowledge the National Cancer Institute Advanced Scientific Computer Laboratory and the National Institutes of Health Division of Computer Research and Technology for computer time and technical assistance.

Received for publication 29 May 1990 and in final form 23 October 1990.

REFERENCES

Ashcroft, F. M. 1987. Adenosine 5'-triphosphate-sensitive potassium channels. *Annu. Rev. Neurosci.* 11:97–118.

Atwater, I., and J. Rinzel. 1986. The β-cell bursting pattern and intracellular calcium. *In* Ionic Channels in Cells and Model Systems, R. Latorre, editor. Plenum Publishing Co., New York. 353–362.

Atwater, I., C. M. Dawson, A. Scott, G. Eddlestone, and E. Rojas. 1980. The nature of the oscillatory behavior in electrical activity for pancreatic β-cell. *Horm. Metab. Res. (Suppl.).* 10:100–107.

Atwater, I., L. Rosario, and E. Rojas. 1983. Properties of calcium-activated potassium channels in the pancreatic β-cell. *Cell Calcium.* 4:451–461.

Bangham, J. A., P. A. Smith, and P. C. Croghan. 1986. Modeling the beta-cell electrical activity. *In* Biophysics of the Pancreatic β-Cell. I. Atwater, E. Rojas, and B. Soria, editors. Plenum Publishing Corp. New York. 265–278.

Barrett, J. N., K. L. Magleby, and B. S. Pallotta. 1982. Properties of single calcium-activated potassium channels in cultured rat muscle. *J. Physiol. (Lond.).* 331:211–230.

Bosco, D., L. Orci, and P. Meda. 1989. Homologous but not heterologous contact increases the insulin secretion of individual pancreatic B-cells. *Exp. Cell Res.* 184:72–80.

Boyd, A. E., A. S. Rajan, and K. L. Gaines. 1989. Regulation of insulin release by calcium. *In* Molecular and Cellular Biology of Diabetes Mellitus. Volume I: Insulin Secretion. B. Draznin, S. Melmed, and D. LeRoith, editors. Alan R. Liss, Inc. New York. 93–105.

Carroll, P. B., A. Sherman, R. Ferrer, A. C. Boschero, J. Rinzel, and I. Atwater. 1990. Modulation of the frequency of glucose-dependent bursts of electrical activity by HCO_3/CO_2 in rodent pancreatic B-cells: experimental and theoretical results. *Eur. Biophys. J.* 18:71–77.

Chay, T. R., and H. S. Kang. 1988. Role of single-channel stochastic noise on bursting clusters of pancreatic β-cells. *Biophys. J.* 54:427–435.

Chay, T. R., and J. Keizer. 1983. Minimal model for membrane oscillations in the pancreatic β-cell. *Biophys. J.* 42:181–190.

Chay, T. R., and Y. S. Lee. 1990. Bursting, beating, and chaos by two functionally distinct inward current inactivations in excitable cells. *In* Mathematical Approaches to Cardiac Arrhythmias. J. Jalife, editor. New York Academy of Sciences. New York. 328-350.

Cook, D. L. 1983. Isolated islets of Langerhans have slow oscillations of electrical activity. *Metabolism.* 32:681–685.

Crowley, M. F., and I. R. Epstein. 1989. Experimental and theoretical studies of a coupled chemical oscillator: phase death, multistability, and in-phase and out-of-phase entrainment. *J. Phys. Chem.* 93:2496–2502.

Dean, P. M., and E. K. Matthews. 1970. Glucose-induced electrical activity in pancreatic islet cells. *J. Physiol. (Lond.).* 210:255–264.

Eddlestone, G. T., and E. Rojas. 1980. Evidence of electrical coupling between mouse pancreatic β-cells. *J. Physiol. (Lond.).* 303:76P–77P.

Eddlestone, G. T., A. Gonçalves, J. A. Bangham, and E. Roja. 1984. Electrical coupling between cells in islets of Langerhans in mouse. *J. Membr. Biol.* 77:1–14.

Falke, L. C., K. D. Gillis, D. M. Pressel, and S. Misler. 1989. 'Perforated patch recording' allows long-term monitoring of metabolite-induced electrical activity and voltage-dependent Ca^{2+} currents in pancreatic islet B cells. *FEBS (Fed. Eur. Biochem. Soc.) Lett.* 251:167–172.

Findlay, I., M. J. Dunne, and O. H. Peterson. 1985. High-conductance K^+ channel in pancreatic islet cells can be activated and inactivated by internal calcium. *J. Membr. Biol.* 83:169–175.

Fitzhugh, R. 1961. Impulses and physiological states in theoretical models of nerve membrane. *Biophys. J.* 1:445–466.

Grapengiesser, E., E. Gylfe, and B. Hellman. 1988. Glucose-induced oscillations of cytoplasmic Ca^{2+} in the pancreatic β-cell. *Biochem. Biophys. Res. Commun.* 151:1299–1304.

Halban, P. A., C. B. Wollheim, B. Blondel, P. Meda, E. N. Niesor, and D. H. Mintz. 1982. The possible importance of contact between pancreatic islet cells for the control of insulin release. *Endocrinology.* 111:86–94.

Henquin, J. C., H. P. Meissner, and W. Schmeer. 1982. Cyclic variations of glucose-induced electrical activity in pancreatic β-cells. *Pfluegers Archiv. Eur. J. Physiol.* 393:322–327.

Keizer, J., and G. Magnus. 1989. ATP-sensitive potassium channel and bursting in the pancreatic β-cell. *Biophys. J.* 56:229–242.

Meda, P., I. Atwater, A. Gonçalves, A. Bangham, L. Orci, and E. Rojas. 1984. The topography of electrical synchrony among

β-cells in the mouse islet of Longerhans. *Q. J. Exp. Physiol.* 69:719–735.

Meda, P., R. M. Santos, and I. Atwater. 1986. Direct identification of electrophysiologically monitored cells within intact mouse islets of Langerhans. *Diabetes.* 35:232–236.

Meissner, H. P. 1976. Electrophysiological evidence for coupling between β cells of pancreatic islets. *Nature (Lond.).* 262:502–504.

Michaels, R. L., and J. D. Sheridan. 1981. Islets of Langerhans: dye coupling among immunocytochemically distinct cell types. *Science (Wash. DC).* 214:801–803.

Michaels, D. C., E. P. Matyas, and J. Jalife. 1986. Dynamic interactions and mutual synchronization of sinoatrial node pacemaker cells. *Circ. Res.* 58:706–720.

Michaels, D. C., E. P. Matyas, and J. Jalife. 1987. Mechanisms of sinoatrial pacemaker synchronization: a new hypothesis. *Circ. Res.* 61:704–714.

Orci, L. 1982. Macro and micro-domains in the endocrine pancreas. *Diabetes.* 31:538–565.

Perez-Armendariz, M., and I. Atwater. 1986. Glucose-evoked changes in $[K^+]$ and $[Ca^{2+}]$ in the intercellular spaces of the mouse islet of Langerhans. *In* Biophysics of the Pancreatic β-Cell. I. Atwater, E. Rojas, and B. Soria editors. Plenum Publishing Co., New York. 31–51.

Perez-Armendariz, M., D. C. Spray, and M. V. L. Bennett. 1991. Biophysical properties of gap junctions between freshly dispersed pairs of mouse pancreatic beta cells. *Biophys. J.* 59:76–92.

Pipeleers, D., P. in't Veld, E. Maes, and M. Van de Winkel. 1982. Glucose-induced insulin release depends on functional cooperation between islet cells. *Proc. Natl. Acad. Sci.* USA. 79:7322–7325.

Rall, W. 1977. Core conductor theory and cable properties of neurons. *In* Handbook of Physiology—The Nervous System, J. M. Brookhart and V. B. Mountcastle, editors. American Physiological Society, Bethesda, MD. 1:39–97.

Rall, W., and I. Segev. 1985. Space-clamp problems when voltage clamping branched neurons with intracellular microelectrodes. *In* Voltage and Patch Clamping with Microelectrodes. T. G. Smith, H. Lecar, S. J. Redman, and P. W. Gage, editors. American Physiological Society, Bethesda, MD. 191–216.

Rinzel, J. 1985. Bursting oscillations in an excitable membrane model. *In* Ordinary and Partial Differential Equations. B. D. Sleeman and R. J. Jarvis, editors. Springer-Verlag New York Inc., New York. 304–316.

Rorsman, P., and G. Trube. 1986. Calcium and delayed potassium currents in mouse pancreatic β-cells under voltage clamp conditions. *J. Physiol. (Lond.).* 374:531–550.

Rosario, L. M., R. M. Santos, D. Contreras, B. Soria, and M. Valdeolmillos. 1990. Glucose-induced oscillations of intracellular Ca^{2+} and membrane potential in single mouse islets of Langerhans. *Biophys. J.* 57:306a. (Abstr.)

Satin, L. S., and D. L. Cook. 1989. Calcium current inactivation in insulin-secreting cells is mediated by calcium influx and membrane depolarization. *Pfluegers Arch. Eur. J. Physiol.* 414:1–10.

Scott, A. M., I. Atwater, and E. Rojas. 1981. A method for the simultaneous measurement of insulin release and β-cell membrane potential in single mouse islets of Langerhans. *Diabetologia.* 21:470–475.

Sherman, A., and J. Rinzel. 1989. Collective properties of insulin-secreting cells. *In* Cell to Cell Signalling: From Experiments to Theoretical Models. A. Goldbeter, editor. Academic Press Limited (AP) London. 61–75.

Sherman, A., J. Rinzel, and J. Keizer. 1988. Emergence of organized bursting in clusters of pancreatic β-cells by channel sharing. *Biophys. J.* 54:411–425.

Smith, P. A., F. M. Ashcroft, and P. Rorsman. 1990. Simultaneous recordings of glucose dependent electrical activity and ATP-regulated K^+-currents in isolated mouse pancreatic β-cells. *FEBS (Fed. Eur. Biochem. Soc.) Lett.* 261:187–190.

Valdeolmillos, M., R. M. Santos, D. Contreras, B. Soria, and L. M. Rosario. 1989. Glucose-induced oscillations of intracellular Ca^{2+} concentration resembling bursting electrical activity in single mouse islets of Langerhans. *FEBS (Fed. Eur. Biochem. Soc.) Lett.* 259:19–23.